

1 Management of solar energy to power electrochemical wastewater 2 treatments.

3 *M. Millán, C.M. Fernández-Marchante, J. Lobato, P. Cañizares, M.A. Rodrigo**

4 Department of Chemical Engineering, Faculty of Chemical Sciences & Technologies,
5 University of Castilla-La Mancha, Av. Camilo José Cela n 12, 13071 Ciudad Real, Spain

6 Abstract

7 In this work, the management of photovoltaic (PV) energy, assisted by a redox flow
8 battery (RFB), for powering an electrochemical advanced oxidation process (EAOP), is
9 evaluated. The storage of surplus energy allows to extend the treatment time overnight
10 and to increase the environmental remediation efficiency during the whole
11 electrochemical treatment. Nevertheless, this work points out that it is important to
12 evaluate the most suitable powering strategy to take advantage of the total solar energy
13 produced. The energy supplied by the PV panels to each system depends on the electrical
14 features of the electrochemical devices (electrooxidation reactor and the RFB) and,
15 especially, on the connection between them (series or parallel). A straightforward
16 coupling (without a targeted regulation of the energy distributed between the EAOP and
17 the RFB) brings out a time-depending and uncontrolled powering. This type of strategy
18 opposes to the smarter regulation of the energy between the EAOP and the RFB by means
19 of a targeted powering to each device. Results show higher remediation degrees when
20 both electrochemical devices are directly coupled in parallel, regardless of the operational
21 mode used (straightforward or targeted) due to lower current densities lead to higher
22 global performances for both electrochemical devices. Nonetheless, it is important to note
23 that the green targeted powering notices higher remediations than the straightforward
24 coupling when the system operates under parallel connection and a RFB control. The

25 lower current densities supplied to the RFB point out higher capacities and, consequently,
26 extend the remediation treatment. Those results shed light on interesting conclusions in
27 terms of green energy use. Furthermore, this software tool allows by means of a simple
28 predictive modelling to optime the operational conditions of electrochemical treatments
29 powered by renewable energies and assisted by energy storage systems.

30 **Keywords**

31 Energy management; solar photovoltaic; electrochemical advanced oxidation processes;
32 redox flow batteries; simulation

33

34 **Highlights**

- 35 - Coupling of PV to RFB and EAOPs extends the duration of treatment.
- 36 - Coupling of PV to RFB and EAOPs increases the total remediation degree
37 reached.
- 38 - Lower current densities show higher remediation degrees per unit of energy
39 supplied.
- 40 - Lower current densities allow to store a large amount of energy.
- 41 - Parallel electrical distributions allow to work under efficient operational
42 conditions.

43

44

45

46 *Corresponding author. Telf: +34 926 295 300; fax: +34 926 295 256. E-mail address:

47 manuel.rodriigo@uclm.es

48 1. Introduction

49 The prevention and reversion of the climate change is, nowadays, one of the main targets
50 of the research community. To overcome the environmental risks that we are facing, the
51 society must learn new sustainable habits. Environmental protection, social cohesion and
52 economic development constitute the three key elements of sustainability [1]. According
53 to that, the term *sustainable development* was defined as “*meeting the needs of the present*
54 *without compromising the ability of the future generations to meet their own needs*” [2].
55 Despite new generations are becoming aware of taking care of the environment, the past
56 uncontrolled industrial and human activities have left high levels of pollution in natural
57 sources including soils and water bodies that may contain hazardous concentrations of
58 persistent organic pollutants (POPs) that should be removed to avoid harmful
59 environmental and human risks.

60 The electrochemical techniques have been proved as one of the most suitable technologies
61 to recover natural sources polluted by a wide range of compounds [3-7]. These processes
62 have been outlined as clean, flexible and powerful, not only for treating wastewater, gases
63 or soils but also for providing drinking water, even from low quality sources [8, 9].
64 Furthermore, it is important to note that those treatments only require electrical energy to
65 operate. Focusing on the treatment of wastewater, electrolyzers equipped with different
66 electrodes materials (platinum, graphite, diamond, mixed metal oxide, metallic dioxide,
67 etc. [10-12]) have demonstrated to be able to promote high degrees of mineralization, as
68 a consequence of the generation of hydroxyl radicals [13], being the diamond one of the
69 most active materials to undergo electrochemical advanced oxidation processes (EAOPs).
70 The conductive diamond electrochemical oxidation (CDEO) has been widely applied by
71 the oxidation of a large diversity of organic pollutant and real wastewater effluents as

72 pharmaceutical [14, 15], petrochemical industry [16], textile industry [17, 18], agriculture
73 [19] or urban wastewater [20, 21].

74 Until now, researchers have aimed their studies at developing efficient technologies
75 capable of recovering affected natural resources, without paying attention to the possible
76 adverse effects of the treatment [22]. Nevertheless, it is essential to strike a balance
77 between efficiency and sustainability when a new treatment is studied to prevent an
78 additional pollution source. Thus, keeping in mind the critical environmental emergency
79 that the humankind must address, and the need for a sustainable development, the concept
80 of green remediation arose. This idea is focused on the recovery of natural sources under
81 the lowest environmental impact [23, 24]. Within this concept, the coupling of
82 electrochemical technologies with renewable energies (REs) could turn these promising
83 treatments into more environmentally friendly processes. It is worth mentioning that
84 electrochemical technologies can be powered indistinctly by the grid or by renewable
85 sources [25, 26] and this later strategy makes them the perfect tandem to get a green
86 remediation. It is worth mentioning that electrochemical technologies can be directly
87 powered by solar panels (Off-grid installations) using direct current (DC) [27]. This
88 operational strategy does not require the use of inverter devices which increases the cost
89 of the remediation setup and its operational management. Furthermore, these
90 characteristics make this operational strategy suitable to be installed in remote areas
91 without energy supply.

92 The use of photovoltaic (PV) energy to power electrochemical treatments has been widely
93 reported in literature, showing promising remediation results [28-34]. Nevertheless, the
94 intermittency and unpredictability that characterize the solar power, increase the
95 treatment time and reduces its efficiency, due to the fluctuating current supplied

96 throughout a day [33]. Despite those negatives operational features, a green powering
97 may be environmental and economically attractive to recover natural sources [35].

98 It has been proved that the use of green energy may work as only power source of batch
99 treatments. Nevertheless, the drawbacks of green energies rule a continuous operation
100 out. To solve this problem, many groups have tested the performance of electrochemical
101 remediation technologies directly coupled with traditional batteries (Lead-acid batteries)
102 directly charged by green energies [36-39]. Nevertheless, a direct powering by batteries
103 may lead to a huge waste of energy due to the efficiencies of energy conversion. To streak
104 a balance between both operational conditions, the use of REs and ESSs under targeted
105 operational conditions is proposed.

106 The control of the current supplied to the electrooxidation treatment avoids undesired
107 reactions, improves the current efficiency, and reduces the energy costs [32].
108 Simultaneously, the storage of exceeding power (typically at midday), by means of ESS
109 working as peak shaving (or load leveling) devices, helps to fit the production and demand
110 of renewable energy [40, 41]. Regarding the ESSs, redox flow batteries (RFBs) have
111 shown promising characteristics regarding other more traditional batteries. The main
112 advantage of the RFBs is that power and energy are independent [42, 43]. This feature
113 provides the RFBs with a high flexibility and allows a straightforward scalability which
114 make easier its coupling to electrochemical technologies. Furthermore, they can directly
115 be powered by renewable energies reaching high storage capacities and efficiencies [44,
116 45]. Thereby, both strategies promote a smother powering, which may turn into efficient
117 remediation treatments.

118 Mathematical models can provide a critical insight into treatment remediation and can
119 work as guide of corrective and preventive actions [46]. Furthermore, these modelling
120 tools may help to improve the electrochemical designs [41] and to assess the best

121 operational conditions. The modelling of electrooxidation treatments has been widely
122 assessed [47-51]. Those studies allow to know in detail the behaviour of **remediation**
123 treatments under different operational conditions. Nonetheless, to the best of our
124 knowledge, studies about the transient response at non-galvanostatic operational mode
125 have not been performed yet.

126 In view of the aforementioned background, the main aim of this work is to test a software
127 tool capable of predicting the degree of remediation reached by an EAOP treatment
128 powered by a combined solar photovoltaic panel and an RFB. Thus, in one of the
129 strategies, the energy produced by the PV panels is straightforwardly used in an
130 electrochemical treatment and stored in **an RFB**. **In turn, the** stored energy is powered **to**
131 **the** environmental treatment overnight. Alternatively, other strategy consisting of the
132 targeted distribution of **solar** energy to the EAOP and RFB. In both cases, the energy
133 distribution between both electrochemical devices (EAOP treatment and redox flow
134 battery) was assessed using different electrical configurations, series and parallel
135 connections, and in three different sunlight profiles corresponding to different seasons of
136 the year. Thus, the best powering strategy was determined according to the highest
137 remediation reached **per unit of energy supplied**, which it is a very important milestone
138 in the search of more sustainable electrochemical advanced oxidation processes for the
139 treatment of wastewater.

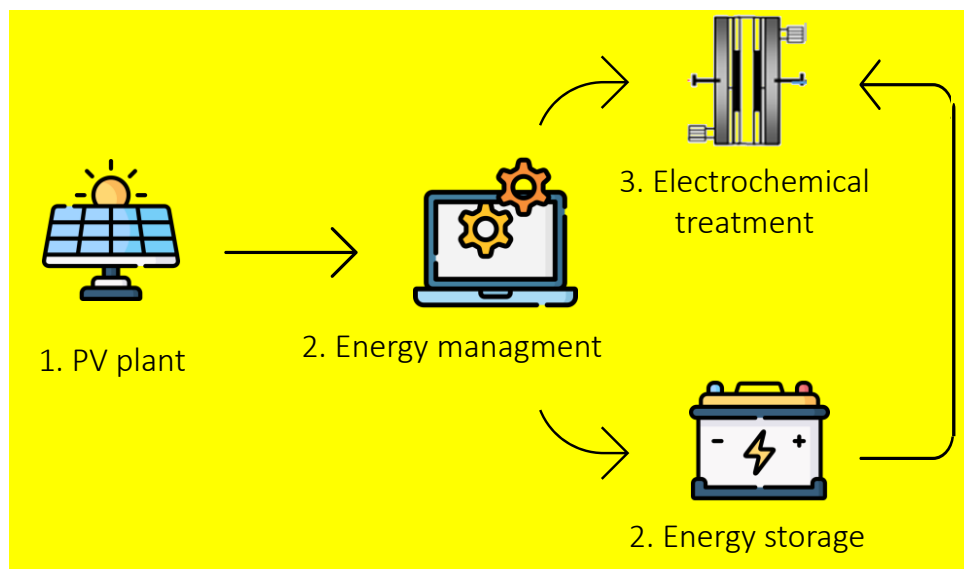
140 **2. Materials and methods**

141 The current density applied highly influences the efficiency of electrochemical
142 remediation treatments [52]. The direct coupling of an electrochemical advanced
143 oxidation **process** (EAOP), such electro-oxidation, with a PV panel does not allow to
144 work under optimum operational conditions because of the fluctuating solar radiations
145 received throughout a day [53, 54].

146 To record and monitor the variables of a treatment is essential to ensure its control and
147 efficiency [55]. Furthermore, to optimize the control of a treatment may bring out
148 operational cost drop and effluent quality increases [56]. Therefore, the control of the
149 energy produced by a PV panel to power an electro-oxidation treatment is essential to
150 reach the most efficient remediation.

151 To overcome this drawback, energy storage systems may be coupled. These devices can
152 provide a smoother powering to the EAOP treatment. Thus, a uniform and more efficient
153 remediation may be carried out. To test this hypothesis, in this work it is simulated the
154 coupling of a vanadium redox flow battery with an EAOP, with the aim of storing the
155 exceeding energy of PV panels at peak hours and powering it at lower or null green power
156 production hours. To perform this simulation, the mathematical modelling of both devices
157 (EAOP and RFB) carried out in a previous study was used. The formulated and tested
158 models were integrated using a simple programming language in Visual Basic and they
159 can be found elsewhere [57]. The fixed parameters of this predictive software tool are
160 related to the specifications of the experimental setups and the variable parameters are
161 the energy flow and the concentration of species which directly depend on the solar
162 radiation received. This model was carried out using experimental bench scale setups
163 coupled with a PV plant made up of two solar panel (1.313 m² each panel) connected in
164 parallel and supplied by ATERSA (Spain). An electrooxidation reactor, DiaCell® 101,
165 provided by Adamant Technologies (Switzerland) and equipped with boron doped
166 diamond (BDD) electrodes (75.8 cm²) supplied by WaterDiam (France) was used as
167 continuous electrochemical remediation system. Furthermore, a homemade vanadium
168 redox flow battery (VRFB) made up of 4 single cells (48 cm² each cell) connected in
169 series was used as electrochemical energy storage system. The RFB operate at 50 mL
170 min⁻¹ using 500 mL of electrolyte solution (1.6 mol dm⁻³ of V⁺ⁿ, 50:50 VO²⁺ and V³⁺).

171 Figure 1 shows a scheme of the modelling software tool which represents the devices that
172 made up the remediation setup. The modelling was carried out considering a synthetic
173 wastewater effluent polluted with 100 mg dm^{-3} of clopyralid and containing 3 g dm^{-3} of
174 Na_2SO_4 as supporting electrolyte. These conditions provide the solution of an initial pH
175 of 3.51 ± 0.19 and an initial conductivity of $4.03 \pm 0.22 \text{ mS cm}^{-1}$. In addition, it is
176 important to take into account that each PV module has an efficiency of 12.14 %
177 according to its technical specifications and the experimental energy efficiency reached
178 by the homemade RFB was around 70 %.



179
180
181

Figure 1. Scheme of the modelling software tool.

182 It is worth mentioning that the energy distribution that **takes** place when two
183 electrochemical devices are coupled is different, according to the electrical connection
184 between them. Furthermore, it is important to note that the energy supplied to each device
185 **directly** depends on the overpotentials of each system and they cannot be controlled.
186 Considering those facts, a targeted powering must be applied to manage and regulate
187 properly the energy supplied to the treatment trying to achieve the most efficient
188 remediation. To assess the most suitable electrical connection, several simulation tests
189 were proposed. **Figure 2** shows the electrical circuits that represent the different electrical

190 connections that could be **conducted** between two electrochemical devices directly
191 coupled to a PV **plant by means of** straightforward or targeted **powerings**. As Figure 1
192 shows, the electrical connection between both electrochemical devices may be performed
193 under series or parallel **configurations**. The energy supplied under a straightforward
194 powering will be distributed according to the internal resistances and **overpotentials** of
195 each device. This distribution will depend on the curves, current-voltage, modelled in a
196 previous work [57]. In contrast, the targeted strategy allows to regulate the energy
197 supplied to each device by means of a variable resistance. Thus, if the variable resistance
198 takes a value of zero, the total solar power will be divided into the EAOP and the RFB,
199 according to a straightforward powering. Conversely, the higher is the current drop
200 induced, the lower is the current supplied to this device. The current distribution will vary
201 according to the electrical configuration as Kirchhoff laws expose [58, 59]. For series
202 circuits, the total potential is the sum of the voltages of each element of the circuit
203 (Equation 1 and 2). By contrast, in parallel circuits, the voltage is the same in all the
204 element into a node (Equation 3 and 4). The resolution procedure is detailed in the
205 Supplementary Material section.

$$206 \quad I_{PV} = I_{EAOP} = I_{RFB} \quad [1]$$

$$207 \quad V_{PV} = V_{EAOP} + V_{RFB} \quad [2]$$

$$208 \quad V_{PV} = V_{EAOP} = V_{RFB} \quad [3]$$

$$209 \quad I_{PV} = I_{EAOP} + I_{RFB} \quad [4]$$

210 According to the previous equations, the series connection allows to power the
211 electrochemical devices at higher current densities. However, this may arise operational
212 drawbacks. Regarding electrochemical remediation treatments, higher currents can
213 involve higher mass transfer limitations [60], because they may turn into parasitic

214 secondary reactions and an efficiency drop [11, 61, 62]. Regarding the RFB charge,
215 higher current densities bring out lower capacities and lower state of charge [63, 64].
216 Consequently, low power could be stored by the system.

217 Considering those **premises**, both electrochemical devices have an optimum overall
218 performance working **at** lower current densities. **Thus, in order to operate under smother**
219 **powering conditions capable of suppling lower current densities to the electrochemical**
220 **systems, a regulated strategy was proposed. To do that,** different resistances were tested
221 with the aim of establishing the most suitable energy management strategy. In contrast to
222 the energy distribution previously described, in this case some features arise due to the
223 inclusion of a new resistance. The resistance simulates a current drop of 25, 50 and 75 %.
224 Equation 5 to 8 show the distribution of current, under series and parallel connections, by
225 means of a EAOP or RFB current control.

226 - *Series connection:*

227 *EAOP control:*
$$I_{PV} = I_{EAOP} + \left(\frac{V_{EAOP}}{R} \right) = I_{RFB} \quad [5]$$

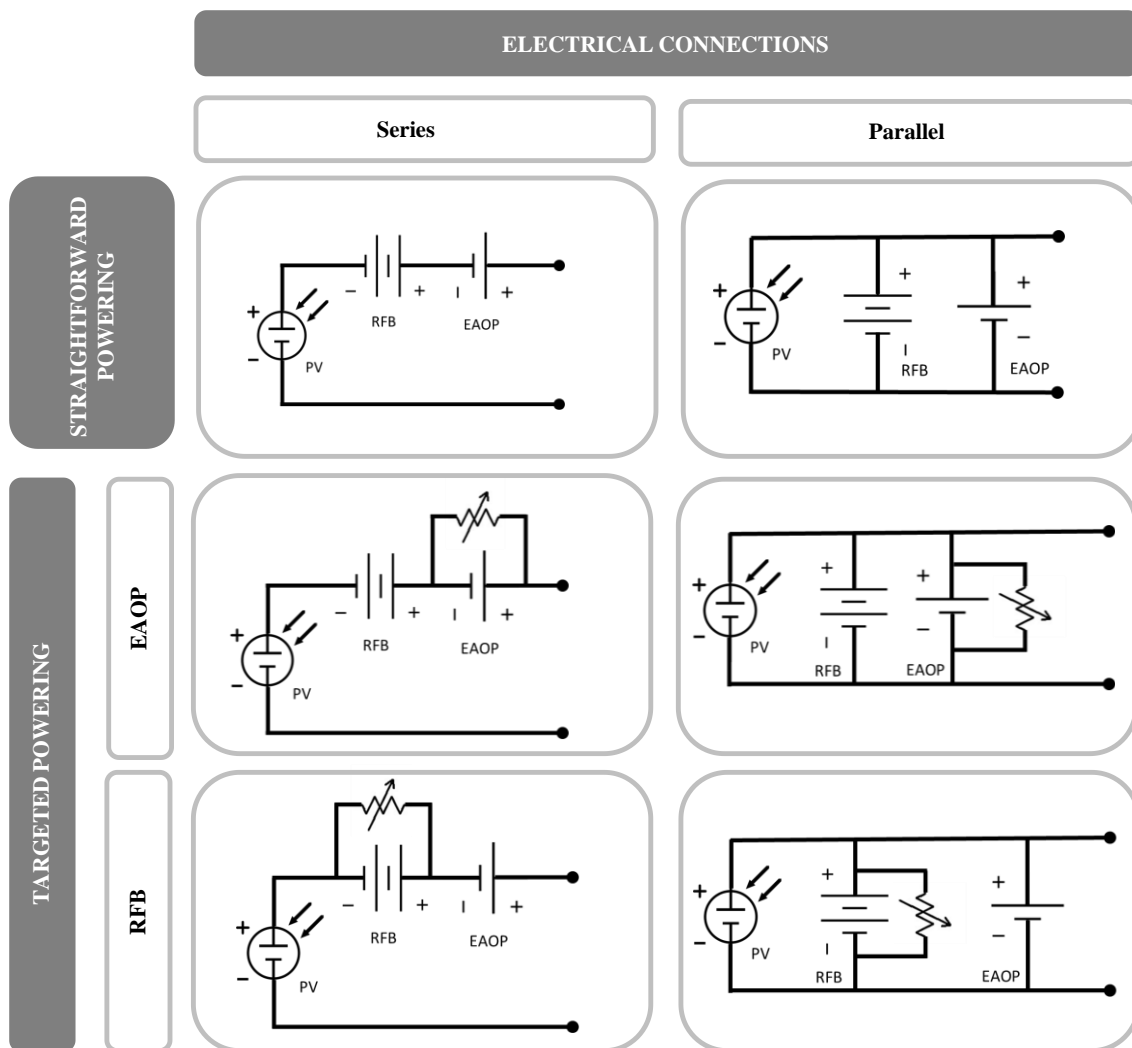
228 *RFB control:*
$$I_{PV} = I_{EAOP} = \left(\frac{V_{RFB}}{R} \right) + I_{RFB} \quad [6]$$

229 - *Parallel connection*

230 *EAOP control:*
$$I_{PV} = I_{EAOP} + \left(\frac{V_{EAOP}}{R} \right) + I_{RFB} \quad [7]$$

231 *RFB control:*
$$I_{PV} = I_{EAOP} + I_{RFB} + \left(\frac{V_{RFB}}{R} \right) \quad [8]$$

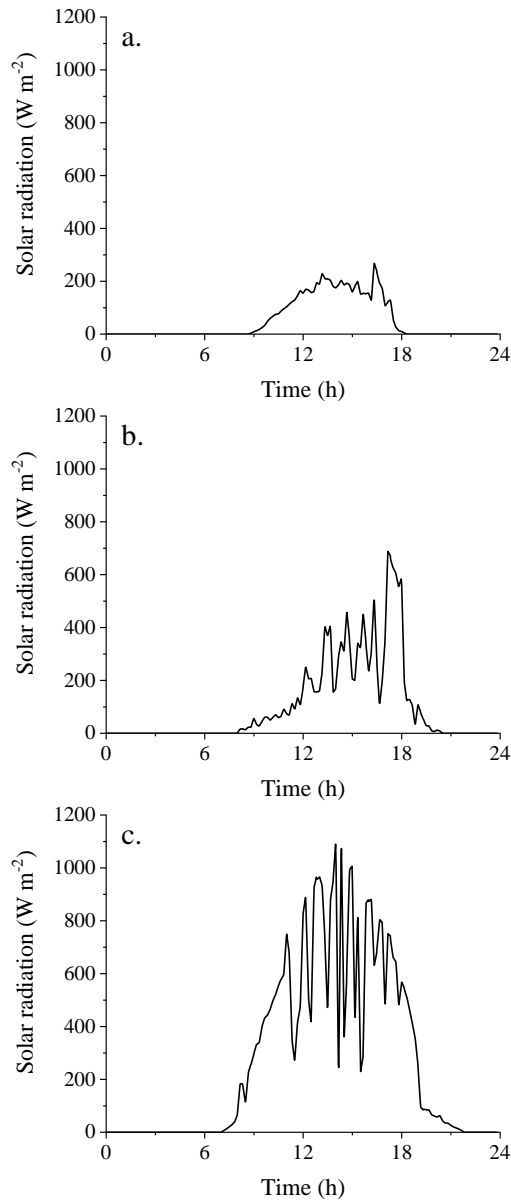
232



233

234 **Figure 2.** Experimental prediction planning. Photovoltaic solar electrochemical oxidation
 235 under straightforward and targeted electrical powering.

236 To test this approach, the remediation of a persistent organic pollutant, clopyralid, was
 237 evaluated according to the proposed electrical connection and considering the models
 238 described elsewhere [57]. Furthermore, this study was performed using three different
 239 solar profiles with the aim of assessing **the efficiency of an assisted photovoltaic solar**
 240 **electrochemical oxidation (PSEO)** treatment under different weather conditions. **Figure 3**
 241 shows the three different solar radiation patterns used, which correspond to typical days
 242 in our location **(3.59N 3.55O)** during the months of January, April and July, representing
 243 different weather conditions within a year.



244

245 **Figure 3.** Solar radiation profiles for three cases of study with different radiation
 246 intensities. Case (a) January, Case (b) April and Case (c) July. **Location: Ciudad Real**
 247 **(3.59 N 3.55 O), Spain.**

248 The average solar radiation received was 51.45, 102.62, 274.28 W m⁻² in January, April
 249 and July, respectively. As expected, the winter day reported the lower total and average
 250 values. Conversely, the sunny day noticed the maximum solar radiation values. It is
 251 important to highlight the lower solar radiation recorded during the first hour of Case (b)

252 regarding Case (a). These differences can be due to earlier cloud covers related to cloudy
253 or rainy days (highly likely in spring).

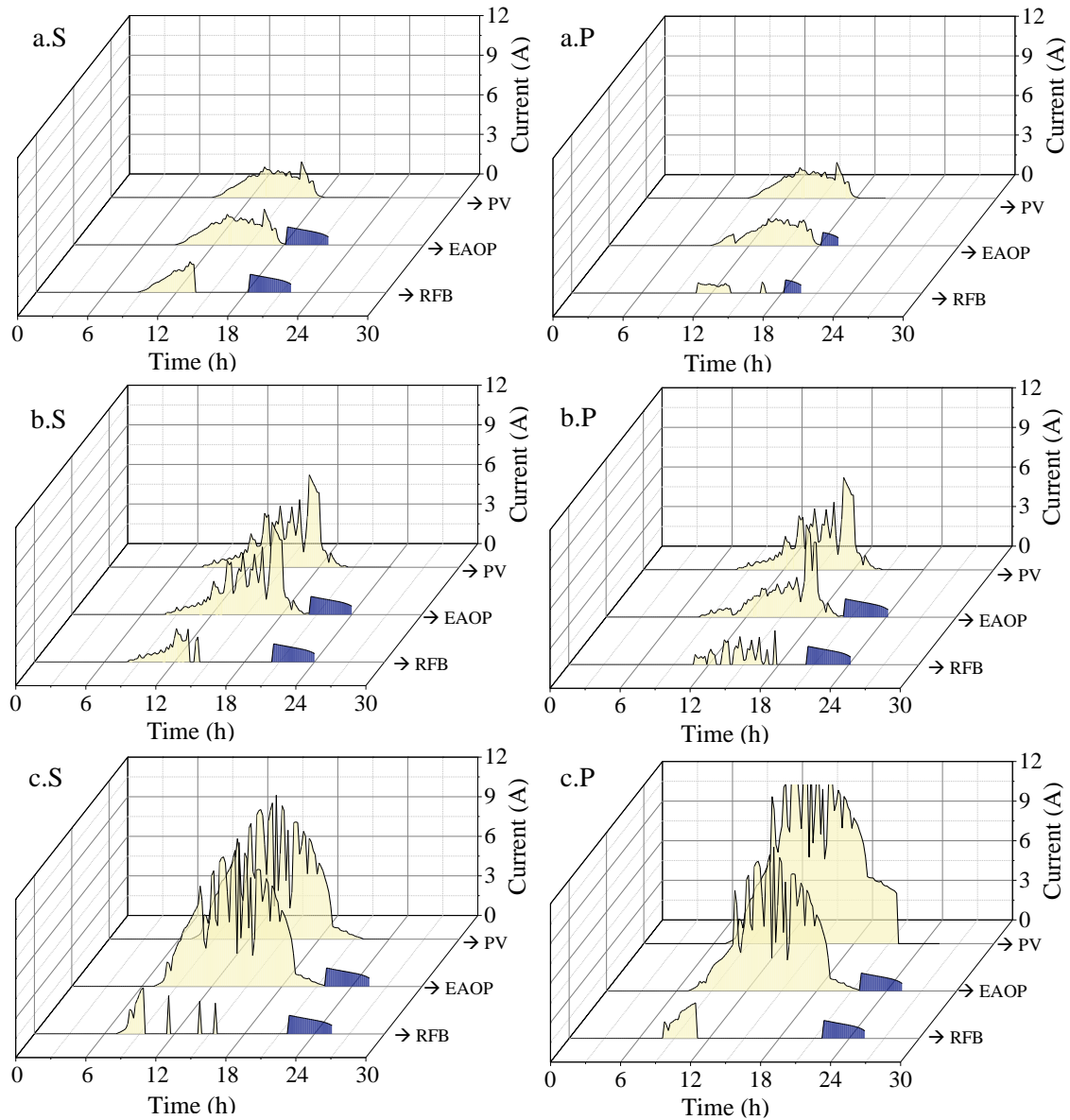
254 **3. Results and discussion**

255 According to the powering strategies proposed and considering the simulation of the
256 models formulated and validated in a previous work of our group [57], the degradation of
257 clopyralid was evaluated for the different powering strategies proposed. Figure 4 shows
258 the current supplied by the PV panels to each electrochemical device under a
259 straightforward series and parallel powering and the current supplied by the RFB to the
260 EAOP at night. As expected, the current supplied by the PV plant to the EAOP and the
261 RFB is the same when the electrochemical devices are connected in series. Conversely,
262 the use of a parallel connection produces a different electric current distribution, as
263 Equation 4 details. Thus, the total current supplied by the PV plant is the sum of the
264 current powered to the EAOP and the RFB.

265 It is worth mentioning that the current supplied to the RFB drops to zero when the battery
266 reaches the full state of charge and, thus, once the battery is completely charged, the total
267 solar power is sent to the EAOP. According to that, the RFB remains under open circuit
268 potential (OCP) until the discharge step takes place. At that moment, the RFB works as
269 power supply of the EAOP. Concerning voltage, the voltage supplied by the PV panel
270 will follow the opposite trend than the current regarding Kirchhoff law. Figure 5 shows
271 the voltage profiles of each device.

272 As expected, faster charge steps are observed when the system is powered under a series
273 configuration due to the higher currents supplied to both electrochemical devices. Despite
274 the charge of the battery can be performed faster at higher current densities, capacity

275 losses may be observed as a consequence of air oxidation, gassing side reactions,
276 vanadium crossover and electrolyte unbalance issues [65, 66].

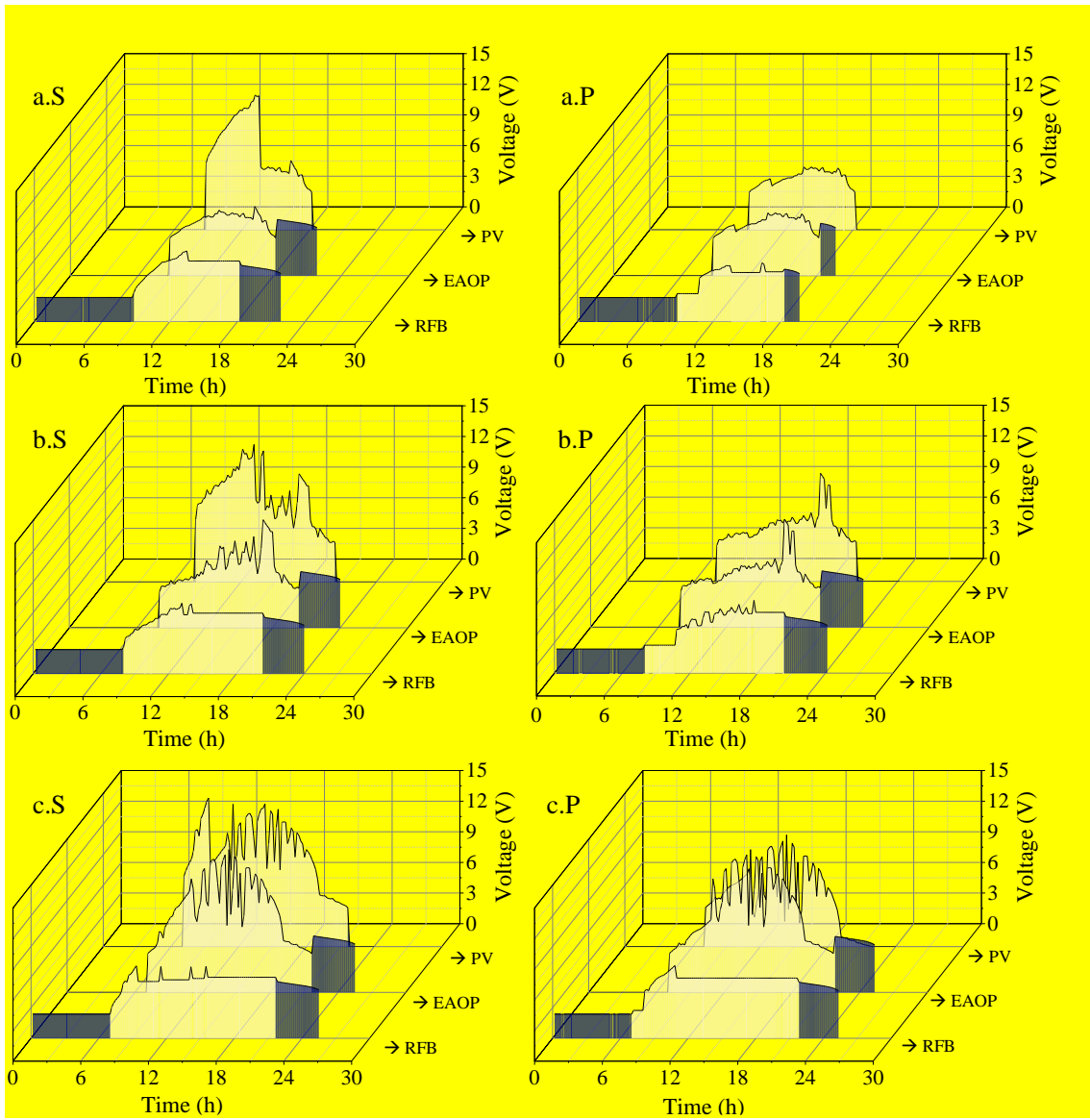


277

278 **Figure 4.** Current flows of the PV plant, the EAOP and the RFB stack under series (S)

279 and parallel (P) electrical connections for the three cases of study (a, b and c Figure 2).

280 Daytime hours (yellow fill) and night hours (blue fill).



281

282 **Figure 5.** Voltage of the PV plant, the EAOP and the RFB stack under series (S) and
 283 parallel (P) electrical connections for the three cases of study (a, b and c Figure 2).
 284 Daytime hours (yellow fill) and night hours (blue fill).

285

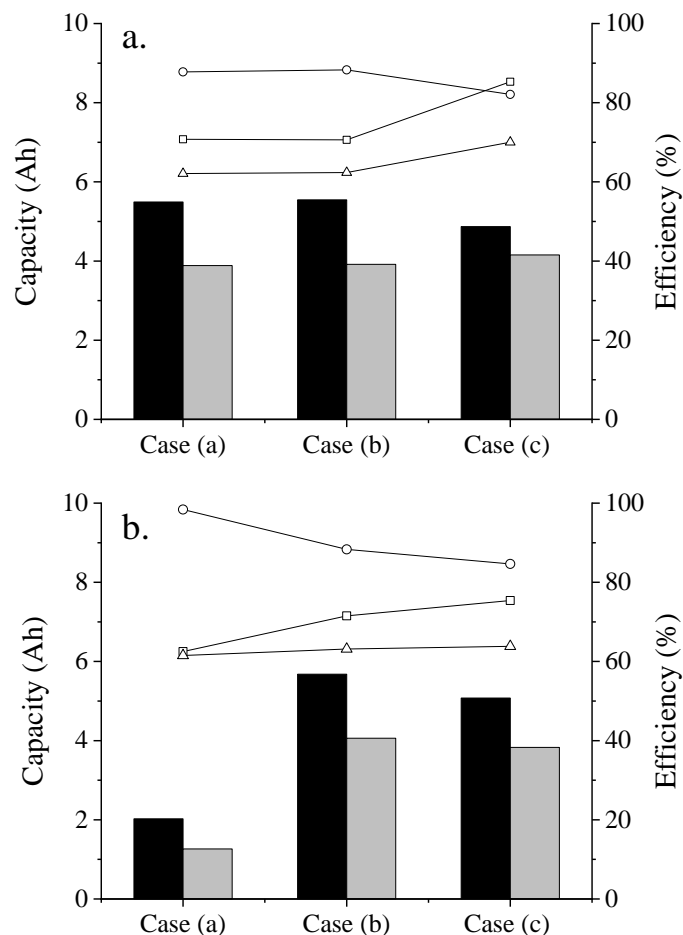
286

287

288

289

290 To evaluate this trend, charge and discharge capacities were quantified. In addition,
 291 coulombic, voltage and energy efficiencies of the battery were calculated as reported
 292 elsewhere [67-69]. Those parameters allow to assess the overall performance of the
 293 battery when it is charged under different weather conditions and electrical
 294 configurations. **Figure 6** shows the charge and discharge capacities, and the efficiencies
 295 of the battery under different **operational conditions**. As expected, the lower is the current
 296 density supplied to the RFB, the higher is the capacity stored into the battery. Thus, the
 297 higher capacities were noticed in Cases (a) and (b) because of the lower solar radiations
 298 received in those simulation tests. It must be highlighted that a slightly higher capacity
 299 was reached in Case (b) due to the lower solar radiation values observed during the first
 300 hour of the day. Conversely, the lowest capacities were observed in Case (c) because of
 301 the huge current densities powered in this case.



303 **Figure 6.** Charge (black bars) and discharge (grey bars) capacities. Coulombic (\square),
304 voltage (\circ) and energy (Δ) efficiencies under a series (a) and parallel (b) powering.

305 Furthermore, it is important to note that higher capacities were observed using parallel
306 connections. The lower current densities supplied under **these** powering strategies turned
307 into higher capacities. Nevertheless, the power supplied in Case (a) was not enough to
308 reach a full state of charge. Using this electrical connection, the battery only **achieved** an
309 open circuit potential (OCP) of 4.87 V. Conversely, the highest OCP was recorded in case
310 (b) under parallel connection, 5.94 V.

311 Regarding efficiencies, the higher coulombic efficiencies were observed when the charge
312 steps were performed at higher current densities. Coulombic efficiencies losses can be
313 caused by side reaction or cross mixing of electrolyte throughout the membrane [70, 71].
314 The species crossover is mainly due to diffusion or migration forces [72]. Nevertheless,
315 those phenomena were not considered into the RFB model outlined elsewhere [57].
316 Conversely, the voltage and energy efficiencies took lower values under those operational
317 conditions. Higher voltage losses can be observed at higher current densities as a
318 consequence of the higher ohmic overpotentials [69]. The same trend was noticed
319 between series and parallel connections. The higher coulombic efficiencies were reported
320 under series connections, because of the higher current densities supplied in this case. In
321 contrast to that, the higher voltage and energy efficiencies were observed when the RFB
322 and the EAOP worked under a parallel powering strategy.

323 Capacity and efficiencies values took values closer to other reported in literature where a
324 RFB was used to store solar power under realistic conditions [44, 73]. Those results
325 suggest again the huge robustness and accuracy of the RFB model previously proposed
326 by our group as reported elsewhere [57].

327 Regarding discharge capacity results, longer remediation treatments could be performed
328 when the battery stores a longer amount of energy. Contrary to expectation, the highest
329 discharge capacities were observed under different electrical connection depending on
330 the season of the year. In Case (b), the battery reached the highest discharge capacity
331 under a parallel connection. Conversely, in Case (c) the battery was able to discharge a
332 higher amount of energy when the electrochemical devices were connected in series.
333 Those differences may be due to the different average current densities between charge
334 and discharge steps, which may turn into different reaction speeds. This could explain the
335 lower coulombic efficiencies obtained, regardless of the operational conditions and the
336 case of study.

337 Many research groups reported the efficiency of an electrochemical remediation process
338 according to the initial pollutant concentration and the current density supplied [21, 74,
339 75]. At high organic concentrations, and low current densities, the pollutant is linearly
340 mineralized following a kinetically controlled process. In contrast to that, at low
341 contaminant concentrations and high current density values, the organic matter
342 concentration drops exponentially, because of mass-transport limitations and side
343 reactions of oxygen evolution. Furthermore, it is claimed that the remediation of
344 concentrated wastewater effluents requires lower specific power consumptions [76, 77].
345 Considering those premises, the removal of clopyralid was evaluated according to the
346 power supplied to the electrooxidation reactor regarding the different powering strategies
347 proposed. It is worth mentioning that the oxidation of clopyralid was evaluated according
348 to Reaction 1. This reaction points out that 18 electrons must be exchanged to mineralize
349 the pollutant model of this study, clopyralid.

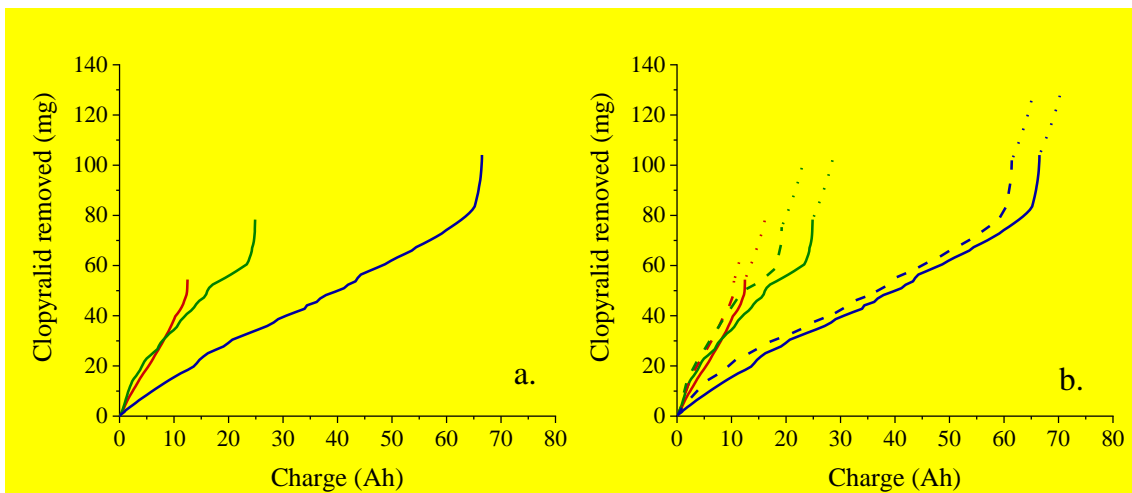


351 The hydroxyl radical that are electrogenerated on the anode surface as Reaction 2 details,
352 attack the pollutant until its complete oxidation up to CO₂.



354 Figure 7 shows the specific clopyralid removal (total clopyralid removed per Ah) under
355 a single PSEO and a PSEO assisted by a RFB by means of a series and parallel
356 straightforward coupling. Figure 7a shows the degradation attained without an energy
357 storage system. In those cases, 54.43, 78.34 and 104.06 mg were removed in Cases (a),
358 (b) and (c), respectively. The longest summer day, and its higher solar radiation, are tied
359 to higher remediation levels. According to the treatment time, the treatment was running
360 14.49 h during the summer day and only 9.33 h the winter day. The higher is the current
361 supplied to the EAOP, the higher is the concentration of oxidants into the bulk solution
362 which may favour the mineralization of organic matter [78].

363 Nevertheless, despite the total solar radiation received in Case (c) was 5.33 times higher
364 than in Case (a), the remediation reached in the first case was only a 43.39 % higher.
365 Regarding the EAOP assisted by the RFB, results show higher remediations regardless
366 the electrical connection used and the treatment day.



367

368 **Figure 7.** Total clopyralid removed under a EAOP powered by a PV plant without (a)
369 and with (b) energy storage. **PV powering:** Series (**solid** line) and parallel (**dashed** line)
370 electrical connections. **RFB powering:** dotted line. Case a (**red**), Case b (**green**) and Case
371 c (**blue**).

372 Figure 5b shows that the use of parallel electrical connections is slightly more efficient in
373 all cases. Nevertheless, the increase of removal was almost the same once the RFB was
374 used. The removal increases up to 48.30, 33.94 and a 68.37 % when the battery was
375 coupled in series. On the other hand, a 19.21, 31.56 and 64.13 % of increase was observed
376 in parallel connection. **Thus, results show that when the battery was completely charge,**
377 **around 25.8 ± 0.5 mg of clopyralid were removed. In these cases, the battery extended**
378 **the treatment around 3.74 ± 0.08 h.** The lowest increase observed in Case (a) under
379 parallel connection could be due to the battery was not able to reach a full state of charge
380 under those operational conditions. Consequently, the energy supplied by the battery was
381 negligible regarding the rest of studies. **In this case, the RFB powering only removed 9.08**
382 **mg of clopyralid. It is important to note that the fluctuating currents supplied to the EAOP**
383 **do not allow to perform the treatment under constant operational conditions and**
384 **consequently, the removal does not reach an equilibrium state. To avoid this problem, a**
385 **smart control of the flow rate must be implemented as it was proved by our group in**
386 **previous studies [52]**

387 To quantify in detail the removal efficiency of the process, the removal per unit of energy
388 was calculated. Table 1 shows the removal of energy per Wh supplied to the EAOP. These
389 results suggest once again that the use of a parallel electrical connection between a EAOP
390 and a RFB directly coupled to a PV panel bring out a more efficient remediation. Despite
391 a lower energy is supplied to both electrochemical devices, the processes work under
392 more suitable operational conditions. Furthermore, it is important to highlight that the

393 best results were reached in Case (a), because of the lower current densities supplied by
 394 the PV panel, associated with the lower solar radiation received. Those results confirm
 395 again the higher efficiency of remediation treatments working at lower current densities.

396 **Table 1.** Removal of clopyralid per unit of energy supplied to the system.

	Removal (mg Clop Wh ⁻¹)		
	Without storage	With energy storage	
		Series	Parallel
Case (a)	0.75	0.87	1.01
Case (b)	0.42	0.50	0.67
Case (c)	0.11	0.18	0.20

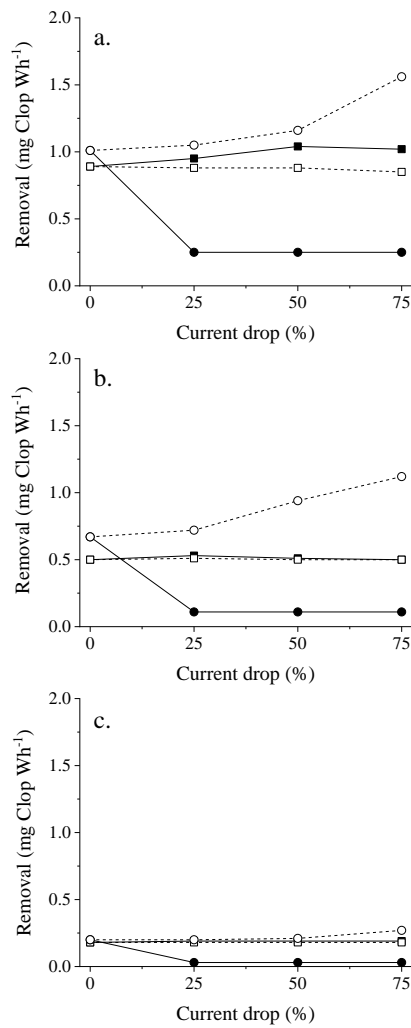
397
 398 According to the previous results, it can be claimed that working at lower current densities
 399 lead to more efficient remediations. Consequently, the use of a straightforward parallel
 400 connection could be an easier operational strategy to reach the most efficient remediation.

401 This statement was also confirmed by other work reported by our group where the PSEO
 402 of a polluted effluent was carried out using a bench scale setup made up of two
 403 electrolyzers [79]. The results reported removal of clopyralid between 0.48 and 2.52 mg
 404 of clopyralid per Wh, being the remediation reached most efficient when both
 405 electrolyzers were connected in parallel to the PV plant. Thus, those results claimed that
 406 lower current densities, as a consequence of parallel connections, bring out efficient
 407 remediations and avoid the waste of green energy.

408 Once known that the parallel configuration leads to a higher remediation performance in
 409 terms of removal of pollutant per unit of energy, the influence of the initial pollutant
 410 concentration was assessed. To do that, predictive analyses were carried out by an initial
 411 pesticide concentration of 10 and 1000 mg dm⁻³. For comparative proposes, Case (b) was

412 selected to undergo this study. Results pointed out a more efficient remediation when the
413 effluent was highly polluted, 1000 mg dm^{-3} , reaching a removal of 2.05 mg of clopyralid
414 per Wh. As expected, the lower the pollutant concentration, the lower the remediation
415 efficiency because of mass transfer problems may arise. Thus, only 0.09 mg of clopyralid
416 per Wh were removed from the effluent polluted with 10 mg dm^{-3} . These results claim
417 that the current supplied by the PV plant and the RFB to the EAOP and the initial pollutant
418 concentration determine the efficiency of an EAOP.

419 To optimize the EAOP, the control of the current supplied to each device was assessed.
420 **Figure 8** shows the removal of clopyralid per unit of energy supplied to the EAOP using
421 a targeted series or electrical connection. As the simulation planning exposed, a current
422 control may be carried out on the remediation treatment or on the battery. Under series
423 electrical connection, the electrochemical device that it is controlled undergoes a current
424 drop. Conversely, the other device is supplied in the same way than under a
425 straightforward series powering. In contrast to the current distribution in series, the use
426 of a controlled parallel powering strategy sends the exceeding energy supplied by the PV
427 panel to the electrochemical devices that is not controlled. Thus, this study allows to strike
428 a balance between the energy supplied to the EAOP and the RFB with the aim of reaching
429 the most efficient remediation.



430

431 **Figure 8.** Removal per unit of energy supply. Series (□) and parallel (○) connection
 432 between a EAOP and a RFB stack. EAOP (full symbol) or RFB (empty symbol) control.
 433 Case (a); Case (b); Case (c).

434 Considering those premises, current drops of a 25, 50 and 75 % were simulated on each
 435 electrochemical device, and under series and parallel connections, with the aim of
 436 evaluating the most effective energy distribution capable of reaching the highest and most
 437 efficient remediation. Furthermore, this prediction was performed for the three cases of
 438 study previously exposed. Results show once again more efficient remediations when the
 439 treatment worked at lower current densities, being this trend more prominent in Case (a).

440 Regarding series connections, slight differences are **observed**. Nevertheless, higher
441 remediations are **achieved** under a EAOP control. As expected, the higher the current
442 drop, the higher the remediation quantified.

443 Those results confirm the lower efficiencies of EAOPs at higher current densities, because
444 of the waste of energy **in** secondary reactions [80]. It is important to highlight that a
445 current drop to the EAOP, when the system works under parallel connection, does not
446 allow the charge of the battery. The drop of current involves lower voltages values. Thus,
447 considering that under parallel connection both devices have the same voltage, those
448 values could be lower than the **overvoltages** of the battery which **does** not provide the
449 electrical feature to carried out the RFB charge. Consequently, the removal reached in
450 those cases is the same than when no energy storage systems are coupled to the EAOP.
451 Simulation data noticed that less than a 10 % of current drop **allows** the charge of the
452 battery.

453 Furthermore, it is worth to mention that the EAOP process reaches the highest
454 remediation when the system works under a parallel connection and an RFB control. The
455 lower current densities supplied to the battery lead to higher capacities which extend the
456 treatment time overnight and increase **the** total pollutant removal. **The lower overvoltages**
457 **reached at low current densities increase the charge voltage window of the battery which**
458 **results into a higher capacity [81]. Consequently, the higher the energy stored, the longer**
459 **the discharge time.**

460 **In short, it is important to highlight that predictive modelling is an innovative and**
461 **promising tool able to optimize the operational condition of treatment in order to increase**
462 **its performance and sustainability.**

463 **4. Conclusions**

464 From this work, the following conclusions can be drawn.

- 465 - The management of energy coming from a PV panel is key to ensure the power
466 supply of an EAOPs coupled with green energy. Regulation of the solar power
467 allows a smoother powering and consequently an efficient remediation. On the
468 other hand, to store exceeded energy **extends** the treatment time.
- 469 - The coupling of a RFB noticeable increases the remediation reached regarding a
470 single PSEO treatment without energy storage.
- 471 - The straightforward powering of a EAOP and an RFB by a PV plant can be
472 performed under series and parallel connections. Results reported higher
473 remediation values when both electrochemical devices are directly coupled in
474 parallel due to the lower current densities supplied to both systems which **turn into**
475 higher overall performances.
- 476 - The green targeted powering allows an exhaustive control of the remediation and
477 storage processes. Results suggest again that the use of a parallel connection under
478 an RFB control aims to a higher remediation. The lower current densities supplied
479 to the RFB **points** out higher capacities which extend the remediation treatment.

480 **Acknowledgments**

481 Financial support from the Spanish Agencia Estatal de Investigación through project
482 PID2019-107271RB-I00 (AEI/FEDER, UE) is gratefully acknowledged. M. Millán
483 thanks the UCLM for the predoctoral contract within the framework of the Plan Propio
484 I+D.

485 **References**

- 486 [1] M. Garrido-Baserba, A. Hospido, R. Reif, M. Molinos-Senante, J. Comas, M. Poch,
487 Including the environmental criteria when selecting a wastewater treatment plant,
488 Environ. Modell. Softw., 56 (2014) 74-82.
- 489 [2] UN, Report of the World Commission on Environment and Development: Our
490 Common Future, <https://www.un.org/>, 1987.
- 491 [3] F.C. Moreira, R.A.R. Boaventura, E. Brillas, V.J.P. Vilar, Electrochemical advanced
492 oxidation processes: A review on their application to synthetic and real wastewaters, App.
493 Catal., B, 202 (2017) 217-261.
- 494 [4] M.A. Rodrigo, N. Oturan, M.A. Oturan, Electrochemically Assisted Remediation of
495 Pesticides in Soils and Water: A Review, Chem. Rev., 114 (2014) 8720-8745.
- 496 [5] C.A. Martinez-Huitle, E. Brillas, Electrochemical alternatives for drinking water
497 disinfection, Angew. Chem. Int. Ed., 47 (2008) 1998-2005.
- 498 [6] K.R. Reddy, C. Cameselle, Electrochemical Remediation Technologies for Polluted
499 Soils, Sediments and Groundwater, Wiley 2009.
- 500 [7] J. Virkutyte, M. Sillanpää, P. Latostenmaa, Electrokinetic Soil Remediation – Critical
501 Overview, Sci. Total. Environ., 289 (2002) 97-121.
- 502 [8] P. Drogui, J.-F. Blais, G. Mercier, Review of Electrochemical Technologies for
503 Environmental Applications, Recent Pat. Eng., 1 (2007) 257-272.
- 504 [9] S. Vasudevan, M.A. Oturan, Electrochemistry: as cause and cure in water pollution—
505 an overview, Environ. Chem. Lett., 12 (2014) 97-108.
- 506 [10] A. Karaçali, M. Muñoz-Morales, S. Kalkan, B.K. Körbahti, C. Saez, P. Cañizares,
507 M.A. Rodrigo, A comparison of the electrolysis of soil washing wastes with active and
508 non-active electrodes, Chemosphere, (2019) 19-26.

- 509 [11] M.A. Rodrigo, P. Cañizares, A. Sánchez-Carretero, C. Sáez, Use of conductive-
510 diamond electrochemical oxidation for wastewater treatment, *Catal. Today*, 151 (2010)
511 173-177.
- 512 [12] A.M. Polcaro, S. Palmas, F. Renoldi, M. Mascia, On the performance of Ti/SnO₂
513 and Ti/PbO₂ anodes in electrochemical degradation of 2-chlorophenol for wastewater
514 treatment, *J. Appl. Electrochem.*, 29 (1999) 147-151.
- 515 [13] T. Muddemann, D. Haupt, M. Sievers, U. Kunz, Electrochemical Reactors for
516 Wastewater Treatment, *ChemBioEng Reviews*, 6 (2019) 142-156.
- 517 [14] I. Sirés, E. Brillas, Remediation of water pollution caused by pharmaceutical residues
518 based on electrochemical separation and degradation technologies: A review, *Environ.*
519 *Int.*, 40 (2012) 212-229.
- 520 [15] J.R. Dominguez, T. Gonzalez, P. Palo, J. Sanchez-Martin, M.A. Rodrigo, C. Saez,
521 Electrochemical Degradation of a Real Pharmaceutical Effluent, *Water Air and Soil*
522 *Pollution*, 223 (2012) 2685-2694.
- 523 [16] E.V. dos Santos, S.F.M. Sena, D.R. da Silva, S. Ferro, A. De Battisti, C.A. Martínez-
524 Huitle, Scale-up of electrochemical oxidation system for treatment of produced water
525 generated by Brazilian petrochemical industry, *Environ. Sci. Pollut. R.*, (2014).
- 526 [17] P.V. Nidheesh, M. Zhou, M.A. Oturan, An overview on the removal of synthetic
527 dyes from water by electrochemical advanced oxidation processes, *Chemosphere*, 197
528 (2018) 210-227.
- 529 [18] C.A. Martínez-Huitle, E. Brillas, Decontamination of wastewaters containing
530 synthetic organic dyes by electrochemical methods: A general review, *App. Catal., B*, 87
531 (2009) 105-145.

532 [19] L. Bu, S. Zhu, S. Zhou, Degradation of atrazine by electrochemically activated
533 persulfate using BDD anode: Role of radicals and influencing factors, *Chemosphere*, 195
534 (2018) 236-244.

535 [20] M.J. Martín de Vidales, M. Millán, C. Sáez, J.F. Pérez, M.A. Rodrigo, P. Cañizares,
536 Conductive diamond electrochemical oxidation of caffeine-intensified biologically
537 treated urban wastewater, *Chemosphere*, 136 (2015) 281-288.

538 [21] M.A. Rodrigo, P. Canizares, C. Buitron, C. Saez, Electrochemical technologies for
539 the regeneration of urban wastewaters, *Electrochim. Acta*, 55 (2010) 8160-8164.

540 [22] C.M. Fernández-Marchante, F.L. Souza, M. Millán, J. Lobato, M.A. Rodrigo,
541 Improving sustainability of electrolytic wastewater treatment processes by green
542 powering, *Sci. Total. Environ.*, 754 (2021).

543 [23] EPA, Introduction to Green Remediation, United States Environmental Protection
544 Agency, [https://www.epa.gov/sites/production/files/2015-](https://www.epa.gov/sites/production/files/2015-04/documents/grn_remed_epa-542-f-08-002.pdf)
545 [04/documents/grn_remed_epa-542-f-08-002.pdf](https://www.epa.gov/sites/production/files/2015-04/documents/grn_remed_epa-542-f-08-002.pdf), 2011.

546 [24] U. EPA, Green Remediation: Incorporating Sustainable Environmental Practices
547 into Remediation of Contaminated Sites, U.S. Environmental Protection Agency, 2008.

548 [25] I. Hassan, E. Mohamedelhasan, E.K. Yanful, Solar powered electrokinetic
549 remediation of Cu polluted soil using a novel anode configuration, *Electrochim. Acta*,
550 181 (2015) 58-67.

551 [26] I. Hassan, Integrated solar electrokinetic remediation of heterogeneous soils
552 contaminated with copper, 2011.

553 [27] K. Baek, X. Mao, A. Ciblak, A.N. Alshawabkeh, Green remediation of soil and
554 groundwater by electrochemical methods, *Geotechnical Special Publication*, 2012, pp.
555 c4348-4357.

556 [28] F. Souza, C. Saéz, J. Llanos, M. Lanza, P. Cañizares, M.A. Rodrigo, Solar-powered
557 CDEO for the treatment of wastewater polluted with the herbicide 2,4-D, *Chem. Eng. J.*,
558 277 (2015) 64-69.

559 [29] E. Alvarez-Guerra, A. Dominguez-Ramos, A. Irabien, Photovoltaic solar electro-
560 oxidation (PSEO) process for wastewater treatment, *Chem. Eng. J.*, 170 (2011) 7-13.

561 [30] J.M. Ortiz, E. Exposito, F. Gallud, V. Garcia-Garcia, V. Montiel, A. Aldaz,
562 Photovoltaic electro dialysis system for brackish water desalination: Modeling of global
563 process, *J. Membr. Sci.*, 274 (2006) 138-149.

564 [31] M. Thomson, D. Infield, A photovoltaic-powered seawater reverse-osmosis system
565 without batteries, *Desalination*, 153 (2003) 1-8.

566 [32] D. Valero, V. García-García, E. Expósito, A. Aldaz, V. Montiel, Electrochemical
567 treatment of wastewater from almond industry using DSA-type anodes: Direct connection
568 to a PV generator, *Sep. Purif. Technol.*, 123 (2014) 15-22.

569 [33] D. Valero, J.M. Ortiz, E. Expósito, V. Montiel, A. Aldaz, Electrochemical
570 Wastewater Treatment Directly Powered by Photovoltaic Panels: Electrooxidation of a
571 Dye-Containing Wastewater, *Environ. Sci. Technol.*, 44 (2010) 5182-5187.

572 [34] D. Marmanis, K. Dermentzis, A. Christoforidis, K. Ouzounis, A. Moutzakis,
573 Electrochemical treatment of actual dye house effluents using electrocoagulation process
574 directly powered by photovoltaic energy, *Desalination Water Treat.*, 56 (2015) 2988-
575 2993.

576 [35] M. Panizza, P.A. Michaud, G. Cerisola, C. Comninellis, Electrochemical treatment
577 of wastewaters containing organic pollutants on boron-doped diamond electrodes:
578 Prediction of specific energy consumption and required electrode area, *Electrochem.*
579 *Commun.*, 3 (2001) 336-339.

580 [36] K. Iyappan, C.A. Basha, R. Saravanathamizhan, N. Vedaraman, C.A. Tahiyah Nou
581 Shene, S.N. Begum, Electrochemical treatment of tannery effluent using a battery
582 integrated DC-DC converter and solar PV power supply--an approach towards
583 environment and energy management, *J. Environ. Sci. Health. A Tox. Hazard. Subst.*
584 *Environ. Eng.*, 49 (2014) 1149-1162.

585 [37] M. Nisha Priya, K. Palanivelu, Electrochemical treatment of reactive dye effluent
586 using solar energy, 2005.

587 [38] J.M. de Melo Henrique, D. de Andrade, E.L. Barros Neto, D.R. da Silva, E.V. dos
588 Santos, Solar-powered BDD-electrolysis remediation of soil washing fluid spiked with
589 diesel, *J. Chem. Technol. Biotechnol.*, 94 (2019) 2999-3006.

590 [39] S. Ganiyu, L.R.D. Brito, E.C.T. De Araújo Costa, E.V. Dos Santos, C.A. Martínez-
591 Huitle, Solar photovoltaic-battery system as a green energy for driven electrochemical
592 wastewater treatment technologies: Application to elimination of Brilliant Blue FCF dye
593 solution, *J. Environ. Chem. Eng.*, 7 (2019).

594 [40] H. Chen, T.N. Cong, W. Yang, C. Tan, Y. Li, Y. Ding, Progress in electrical energy
595 storage system: A critical review, *Prog. Nat. Sci.*, 19 (2009) 291-312.

596 [41] S. Bebelis, K. Bouzek, A. Cornell, M.G.S. Ferreira, G.H. Kelsall, F. Lapique, C.P.
597 de Leon, M.A. Rodrigo, F.C. Walsh, Highlights during the development of
598 electrochemical engineering, *Chem. Eng. Res. Des.*, 91 (2013) 1998-2020.

599 [42] W. Wang, Q. Luo, B. Li, X. Wei, L. Li, Z. Yang, Recent Progress in Redox Flow
600 Battery Research and Development, *Adv. Funct. Mater.*, 23 (2012) 970-986.

601 [43] F. Pan, Q. Wang, Redox Species of Redox Flow Batteries: A Review, *Molecules*, 20
602 (2015) 20499-20517.

603 [44] R. López-Vizcaíno, E. Mena, M. Millán, M.A. Rodrigo, J. Lobato, Performance of
604 a vanadium redox flow battery for the storage of electricity produced in photovoltaic solar
605 panels, *Renew. Energ.*, 114 (2017) 1123-1133.

606 [45] E. Mena, R. López-Vizcaíno, M. Millán, P. Cañizares, J. Lobato, M.A. Rodrigo,
607 Vanadium redox flow batteries for the storage of electricity produced in wind turbines,
608 *Int. J. Energy Res.*, 42 (2018) 720-730.

609 [46] X. Shen, D. Lampert, S. Ogle, D. Reible, A software tool for simulating contaminant
610 transport and remedial effectiveness in sediment environments, *Environ. Modell. Softw.*,
611 109 (2018) 104-113.

612 [47] A. Urriaga, C. Fernández-González, S. Gómez-Lavín, I. Ortiz, Kinetics of the
613 electrochemical mineralization of perfluorooctanoic acid on ultrananocrystalline boron
614 doped conductive diamond electrodes, *Chemosphere*, 129 (2015) 20-26.

615 [48] O. Scialdone, A. Galia, S. Randazzo, Electrochemical treatment of aqueous solutions
616 containing one or many organic pollutants at boron doped diamond anodes. Theoretical
617 modeling and experimental data, *Chem. Eng. J.*, 183 (2012) 124-134.

618 [49] M. Panizza, A. Kapalka, C. Comninellis, Oxidation of organic pollutants on BDD
619 anodes using modulated current electrolysis, *Electrochim. Acta*, 53 (2008) 2289-2295.

620 [50] A.M. Polcaro, M. Mascia, S. Palmas, A. Vacca, Kinetic Study on the Removal of
621 Organic Pollutants by an Electrochemical Oxidation Process, *Ind. Eng. Chem. Res.*, 41
622 (2002) 2874-2881.

623 [51] A. Kapalka, G. Fóti, C. Comninellis, Kinetic modeling of the Electrochemical
624 mineralization of organic pollutants for wastewater treatment, *J. Appl. Electrochem.*, 38
625 (2008) 7-16.

626 [52] M. Millán, M.A. Rodrigo, C.M. Fernández-Marchante, P. Cañizares, J. Lobato,
627 Powering with Solar Energy the Anodic Oxidation of Wastewater Polluted with
628 Pesticides, *ACS Sustain. Chem. Eng.*, 7 (2019) 8303-8309.

629 [53] M.R. Islam, F. Rahman, W. Xu, *Advances in Solar Photovoltaic Power Plants*,
630 Springer Berlin Heidelberg 2016.

631 [54] W. Cao, Y. Hu, *Renewable Energy: Utilisation and System Integration*,
632 IntechOpen 2016.

633 [55] J. Baeza, D. Gabriel, J. Lafuente, An expert supervisory system for a pilot WWTP,
634 *Environ. Modell. Softw.*, 14 (1999) 383-390.

635 [56] J. Guerrero, A. Guisasola, R. Vilanova, J.A. Baeza, Improving the performance of a
636 WWTP control system by model-based setpoint optimisation, *Environ. Modell. Softw.*,
637 26 (2011) 492-497.

638 [57] M. Millán, C.M. Fernández-Marchante, J. Lobato, P. Cañizares, M.A. Rodrigo,
639 Modelling of the treatment of wastewater by photovoltaic solar electrochemical oxidation
640 (PSEO) assisted by redox-flow batteries, *Journal of Water Process Engineering*, 40
641 (2021) 101974.

642 [58] W.R. Browne, *Electrochemistry*, Oxford University Press 2018.

643 [59] S.N. Lvov, *Introduction to Electrochemical Science and Engineering*, Taylor &
644 Francis 2014.

645 [60] A.H. Ltaïef, A. D'Angelo, S. Ammar, A. Gadri, A. Galia, O. Scialdone,
646 Electrochemical treatment of aqueous solutions of catechol by various electrochemical
647 advanced oxidation processes: Effect of the process and of operating parameters, *J.*
648 *Electroanal. Chem.*, 796 (2017) 1-8.

649 [61] M.A. Oturan, J.-J. Aaron, Advanced Oxidation Processes in Water/Wastewater
650 Treatment: Principles and Applications. A Review, Crit. Rev. Env. Sci. Technol., 44
651 (2014) 2577-2641.

652 [62] M. Panizza, G. Cerisola, Direct And Mediated Anodic Oxidation of Organic
653 Pollutants, Chem. Rev., 109 (2009) 6541-6569.

654 [63] Á. Cunha, J. Martins, N. Rodrigues, F.P. Brito, Vanadium redox flow batteries: a
655 technology review, Int. J. Energy Res., 39 (2015) 889-918.

656 [64] K. Lourenssen, J. Williams, F. Ahmadpour, R. Clemmer, S. Tasnim, Vanadium
657 redox flow batteries: A comprehensive review, J. Energy Storage, 25 (2019).

658 [65] M. Skyllas-Kazacos, M. Kazacos, State of charge monitoring methods for vanadium
659 redox flow battery control, J. Power Sources, 196 (2011) 8822-8827.

660 [66] T. Jirabovornwisut, A. Arpornwichanop, A review on the electrolyte imbalance in
661 vanadium redox flow batteries, Int. J. Hydrogen Energy, 44 (2019) 24485-24509.

662 [67] Y. Shi, C. Eze, B. Xiong, W. He, H. Zhang, T.M. Lim, A. Ukil, J. Zhao, Recent
663 development of membrane for vanadium redox flow battery applications: A review, Appl.
664 Energ., 238 (2019) 202-224.

665 [68] X. Ma, H. Zhang, C. Sun, Y. Zou, T. Zhang, An optimal strategy of electrolyte flow
666 rate for vanadium redox flow battery, J. Power Sources, 203 (2012) 153-158.

667 [69] H.J. Lee, N.H. Choi, H. Kim, Analysis of Concentration Polarization Using UV-
668 Visible Spectrophotometry in a Vanadium Redox Flow Battery, J. Electrochem. Soc., 161
669 (2014) A1291-A1296.

670 [70] C. Blanc, A. Rufer, Understanding the Vanadium Redox Flow Batteries, 2010.

671 [71] D.-J. Park, K.-S. Jeon, C.-H. Ryu, G.-J. Hwang, Performance of the all-vanadium
672 redox flow battery stack, J. Ind. Eng. Chem., 45 (2017) 387-390.

673 [72] M. Moazzam, K. Oh, G. Gwak, H. Ju, Water crossover phenomena in all-vanadium
674 redox flow batteries, *Electrochim. Acta*, 297 (2019) 101-111.

675 [73] J. Lobato, E. Mena, M. Millán, Improving a Redox Flow Battery Working under
676 Realistic Conditions by Using of Graphene based Nanofluids, *ChemistrySelect*, 2 (2017)
677 8446-8450.

678 [74] M. Panizza, G. Cerisola, Application of diamond electrodes to electrochemical
679 processes, *Electrochim. Acta*, 51 (2005) 191-199.

680 [75] C. Comninellis, A. Kapalka, S. Malato, S.A. Parsons, L. Poulios, D. Mantzavinos,
681 Advanced oxidation processes for water treatment: advances and trends for R&D, *J.*
682 *Chem. Technol. Biotechnol.*, 83 (2008) 769-776.

683 [76] G. Acosta-Santoyo, J. Llanos, A. Raschitor, E. Bustos, P. Cañizares, M.A. Rodrigo,
684 Performance of ultrafiltration as a pre-concentration stage for the treatment of
685 oxyfluorfen by electrochemical BDD oxidation, *Sep. Purif. Technol.*, 237 (2020) 116366.

686 [77] J. Llanos, A. Raschitor, P. Cañizares, M.A. Rodrigo, Exploring the applicability of
687 a combined electrodialysis/electro-oxidation cell for the degradation of 2,4-
688 dichlorophenoxyacetic acid, *Electrochim. Acta*, 269 (2018) 415-421.

689 [78] A. Dominguez-Ramos, R. Aldaco, A. Irabien, Photovoltaic solar electrochemical
690 oxidation (PSEO) for treatment of liginosulfonate wastewater, *J. Chem. Technol.*
691 *Biotechnol.*, 85 (2010) 821-830.

692 [79] M. Millán, V.M. García-Orozco, J. Lobato, C.M. Fernández-Marchante, G. Roa-
693 Morales, I. Linares-Hernández, R. Natividad, M.A. Rodrigo, Toward more sustainable
694 photovoltaic solar electrochemical oxidation treatments: Influence of hydraulic and
695 electrical distribution, *J. Environ. Manage.*, 285 (2021).

696 [80] C. Comninellis, G. Chen, *Electrochemistry for the Environment*, Springer New
697 York 2009.

698 [81] X. Xi, X. Li, C. Wang, Q. Lai, C. Yuanhui, W. Zhou, C. Ding, Impact of Proton
699 Concentration on Equilibrium Potential and Polarization of Vanadium Flow Batteries,
700 ChemPlusChem, 80 (2015).

701